TURBULENT ROUGH BED BOUNDARY LAYERS IN THE PRESENCE OF NON-LINEAR SURFACE WAVES

M.A. Cotton and P.K. Stansby
Hydrodynamics Research Group, School of Engineering,
University of Manchester, Manchester M13 9PL, U.K.

ABSTRACT

Wind-generated surface waves give rise to the development of periodic unsteady boundary layers on the sea bed. Naturally-occurring waves may have highly non-linear characteristics which will affect the boundary layer through the action of the horizontal pressure gradient at the bed. The frictional characteristics of the boundary layer will, in turn, influence the subsequent evolution of a wave, causing the dissipation of wave energy and hence wave attenuation. In the present work we investigate the effect of a periodic (but non-sinusoidal) pressure gradient 'input' to the calculation of turbulent flow over a rough bed. A k-ε turbulence closure is used to obtain values for the wave friction factor, f_w and wave energy dissipation factor, f_e for different values of the relative roughness a/k_s, where a is the amplitude of fluid motion at the bed and k_s is the Nikuradse equivalent sand roughness of the bed. At given a/k_s the importance of wave non-linearity effects is examined for different values of H/d and d/L, where H is the peak-to-trough wave height, d is the water depth, and L is the wavelength. In the final part of the paper the propagation of wave power is considered in relation to the computed values of f_e.

1. INTRODUCTION

Wave boundary layers in the absence of current action may be characterized as oscillatory flows driven by a time-dependent pressure gradient with zero mean. Two measures of the frictional properties of the flow are generally considered in relation to sediment transport and wave attenuation: these respectively are the peak bed shear stress, $\tau_{b,max}$, and the cycle-averaged rate of energy dissipation, $\overline{\tau_b.u_0}$, where u_0 denotes bed velocity outside the boundary layer. Non-dimensional friction factors, namely the 'wave friction factor' and the 'wave energy dissipation factor', are then defined as

$$f_w = \tau_{b,max}/(\tfrac{1}{2}\rho u_{0,max}^2) \qquad (1)$$

and

$$f_e = \overline{\tau_b.u_0}/[(2/3\pi)(\rho u_{0,max}^3)] \qquad (2)$$

(see for example Fredsøe and Deigaard, 1992). Under linear (i.e. sinusoidal, or *linearized*) conditions the friction factors at high Reynolds numbers are functions of the relative roughness only and, furthermore, f_w and f_e are equal if the friction velocity varies as a pure sinusoid in phase with the free stream (Justesen, 1988). Correlations, such as the one proposed by Nielsen (1992), may then be used to relate the friction factors to a/k_s:

$$f_e = f_w = \exp\left[5.5\left(\frac{a}{k_s}\right)^{-0.2} - 6.3\right] \qquad (3)$$

In the non-linear case, by contrast, f_w and f_e are additionally functions of the wave parameters H/d and d/L; it is also shown below that f_e may be considerably smaller than f_w (a low value of f_e will act to maintain the power a wave transmits cycle-on-cycle).

Previous computational work on wave boundary layers over rough surfaces includes both studies of the linear case with a sinusoidal pressure gradient and also at least one investigation of non-linear effects. In terms of linear waves Fredsøe (1984) assumed a logarithmic velocity profile and proceeded to generate numerical solutions to the unsteady momentum equation, while Justesen (1988) produced numerical results using a k-ε turbulence model. Both authors reported satisfactory agreement with the experimental data for f_w (with $a/k_s \geq 30$) obtained by Kamphuis (1975) using an

oscillating water tunnel. Fredsøe and Deigaard (1992) examined a saw-tooth non-linear wave over a rough bed and found close agreement between the logarithmic velocity profile approach of Fredsøe (1984) and turbulence model calculations. A larger body of work exists for unsteady flows over smooth surfaces: here the review paper of Brereton and Mankbadi (1995) provides a useful introduction. We also note the recent work of Tanaka et al. (1998) who presented experimental data and low-Reynolds-number turbulence model calculations for smooth bed boundary layers generated by non-linear waves.

In the present paper the potential flow analysis of Rienecker and Fenton (1981) is used to generate non-linear wave characteristics. A high-Reynolds-number k-ε model is employed to compute the rough bed boundary layer and values of f_w and f_e are obtained for a range of relative roughnesses, wave height to water depth ratios, and depth to wavelength ratios. Calculated values of the wave energy dissipation factor are used to examine different patterns of wave power propagation in the linear and non-linear cases.

2. WAVE MECHANICS

2.1 Linear Theory

In classical linear wave theory the horizontal pressure gradient is equal to the unsteady flow acceleration in accordance with the non-advective Euler equation:

$$\frac{\partial u}{\partial t} = -\frac{1}{\rho}\frac{\partial p}{\partial x} \tag{4}$$

All velocities are pure harmonic variations and hence the phase-averaged horizontal (x-direction) velocity may be written

$$u(x, z, t) = \alpha(z) \cos(\kappa x - \omega t) \tag{5}$$

where the vertical coordinate, z is measured from the bed. Taking a horizontal reference position x = 0 the velocity at the bed is obtained as

$$u_0 = a\omega \cos \omega t \tag{6}$$

where the particle amplitude at the bed is given by

$$a = \frac{H}{2\sinh(2\pi d/L)} \tag{7}$$

Pressure gradient at the bed is found as

$$\left(-\frac{1}{\rho}\frac{\partial p}{\partial x}\right)_0 = -a\omega^2 \sin \omega t \tag{8}$$

The wave power (or mean energy flux) per unit span is defined as

$$E_f = \overline{\int_0^{\eta}\left(p + \frac{1}{2}\rho\left(u^2 + w^2\right) + \rho g\left(z - d\right)\right) u \, dz} \tag{9}$$

where η is the free surface elevation above the bed and the overbar denotes an average over one cycle. Under linear conditions Equation (9) is evaluated as

$$E_f = \left(\frac{1}{8}\rho g H^2\right)\frac{c}{2}\left(1 + \frac{2\kappa d}{\sinh(2\kappa d)}\right) \tag{10}$$

2.2 Non-Linear Theory

In the approach of Rienecker and Fenton (1981) the governing equations are still cast in potential flow form, but solution is now obtained using Fourier series; the only approximation in the method arises from the truncation of the series to a finite number of terms. In the present adaption (due to Buss and Stansby, 1982) H, T, and d are supplied and wavelength is a result of the calculation. The Fourier series extends to 30 terms. Equation (4) now includes the advective terms so that pressure gradient is determined as

$$\frac{Du}{Dt} = \frac{\partial u}{\partial t} + u\frac{\partial u}{\partial x} + w\frac{\partial u}{\partial z} = -\frac{1}{\rho}\frac{\partial p}{\partial x} \tag{11}$$

Impermeability sets w = 0 at the bed, and further given that

$$u(x, z, t) = \sum_{n=1}^{N} \alpha_n(z) \cos\left[n(\kappa x - \omega t)\right] \tag{12}$$

it follows that

$$\frac{\partial u}{\partial x} = -\frac{1}{c}\frac{\partial u}{\partial t} \tag{13}$$

The non-linear equivalent of Equation (8) is therefore

$$\left(-\frac{1}{\rho}\frac{\partial p}{\partial x}\right)_0 = \left(1 - \frac{u_0}{c}\right)\left(\frac{\partial u}{\partial t}\right)_0 \tag{14}$$

Wave power is determined directly from Equation (9).

3. THE BOUNDARY LAYER MODEL

The boundary layer is driven by the action of a pressure gradient as determined from wave theory: $(-1/\rho)\partial p/\partial x$ is given by Equation (8) in the linear case and by Equation (14) in the non-linear case. The difference in the linear and non-linear treatments of the boundary layer lies in the prescription of the differential operator D/Dt: in the linear case we have simply

$$\frac{D}{Dt} \equiv \frac{\partial}{\partial t} \tag{15}$$

whereas in the non-linear case we may use Equation (13) to write

$$\frac{D}{Dt} \equiv \frac{\partial}{\partial t} + u\frac{\partial}{\partial x} + w\frac{\partial}{\partial z} \equiv \left(1 - \frac{u}{c}\right)\frac{\partial}{\partial t} + w\frac{\partial}{\partial z} \tag{16}$$

where the vertical phase-averaged velocity is obtained from continuity as

$$w = -\int_0^z \frac{\partial u}{\partial x}\,dz = \frac{1}{c}\int_0^z \frac{\partial u}{\partial t}\,dz \qquad (17)$$

Thus, given the two alternative definitions of Equations (15) and (16), it is now possible to devise an otherwise common treatment of the boundary layer.

A standard high-Reynolds-number k-ε turbulence model (see for example Rodi, 1993) is used to compute the oscillatory boundary layer. Thus, the momentum equation and k- and ε-equations read

$$\frac{Du}{Dt} = -\frac{1}{\rho}\frac{\partial p}{\partial x} + \frac{\partial}{\partial z}\left[(\nu + \nu_t)\frac{\partial u}{\partial z}\right] \qquad (18)$$

$$\frac{Dk}{Dt} = P + \frac{\partial}{\partial z}\left[\left(\nu + \frac{\nu_t}{\sigma_k}\right)\frac{\partial k}{\partial z}\right] - \varepsilon \qquad (19)$$

$$\frac{D\varepsilon}{Dt} = C_{\varepsilon 1}\frac{\varepsilon}{k}P + \frac{\partial}{\partial z}\left[\left(\nu + \frac{\nu_t}{\sigma_\varepsilon}\right)\frac{\partial \varepsilon}{\partial z}\right] - C_{\varepsilon 2}\frac{\varepsilon^2}{k} \qquad (20)$$

where

$$\nu_t = C_\mu \frac{k^2}{\varepsilon};\quad P = \nu_t\left(\frac{\partial u}{\partial z}\right)^2;$$
$$C_\mu = 0.09;\ C_{\varepsilon 1} = 1.44;\ C_{\varepsilon 2} = 1.92;\ \sigma_k = 1.0;\ \sigma_\varepsilon = 1.3 \qquad (21)$$

The lower boundary condition on the velocity field is supplied by the standard law-of-the-wall for fully rough turbulent boundary layers (Schlichting, 1979):

$$u^+ = \frac{|u_1|}{u_\tau} = \frac{1}{\kappa}\ln\left(\frac{z_1}{k_s}\right) + 8.5 \qquad (22)$$

with $\kappa = 0.435$. At the first turbulence node above the bed k and ε are specified as

$$k_{1(t)} = \frac{u_\tau^2}{C_\mu^{1/2}};\quad \varepsilon_{1(t)} = \frac{u_\tau^3}{\kappa z_{1(t)}} \qquad (23)$$

Zero gradient conditions are applied to u and k at the top of the solution domain; ε is set to a finite value following Rodi (1993), however the alternative use of a zero gradient condition had a negligible effect upon results. It was found that reduction of κ to a value of 0.4 could increase friction factors by 3 - 4%; a test of a refined law-of-the-wall due to Sajjadi and Aldridge (1995) produced changes in f_w and f_e of the order of only 0.01% (such insensitivity is a consequence of the high k_s^+ values typical of the present wave boundary layers).

The numerical procedures are developed from a scheme by Stansby (1997) which employs a staggered grid for the turbulence field and a parabolic transformation to give high resolution of the near-bed flow. The first velocity node is always located to simultaneously satisfy two criteria:

$$30 \le z^+_{1,max} \le 100 \quad \text{and} \quad 0.03 \le \frac{z_1}{k_s} \le 0.1 \qquad (24)$$

A series of numerical sensitivity tests was undertaken: the most notable finding was that friction factors could vary by approximately ± 2% while the positioning of z_1 satisfied the dual constraints of Equation (24).

4. RESULTS

The waves examined in the present study are characterized by height to depth ratios of H/d = 0.3, 0.45, and 0.6; depth to wavelength ratios are principally within the limits $0.05 \le d/L \le 0.1$. Boundary layer relative roughnesses of $a/k_s = 30$, 100, and 1000 are considered over the full range of wave parameters. Particular attention is paid to case of H/d = 0.6 with $a/k_s = 100$.

Focusing initially on the wave calculation, Figure 1 shows the linear and non-linear free surface profiles for the case H/d = 0.6 and d/L = 0.075. The normalization employed yields simply $(\eta - d)/H = 0.5 \cos \omega t$ for the linear case, however the non-linear profile is distinctly peaked, with $(\eta - d)/H$ exhibiting a maximum of 0.81 and a minimum of –0.19 (note that the cycle-mean surface elevation in both cases is equal to the still water level). Figure 2 shows the corresponding acceleration at the bed. Values are normalized by the peak linear acceleration and hence the linear variation of $(\partial u/\partial t)_0$ is obtained as –sin ωt. Two curves are shown for the non-linear case: the solid line shows $(Du/Dt)_0$, which corresponds to the right hand side of Equation (14); the chain-linked line shows $(\partial u/\partial t)_0$. The non-linear curves display an initial sharp deceleration which is succeeded by a relatively quiescent transition to acceleration and a 'mirror image' sharp acceleration. Linear $(\partial u/\partial t)_0$ and non-linear $(Du/Dt)_0$ provide the input to the boundary layer computation (cf. Equations (8) and (14)).

Wave power as defined by Equation (9) may be normalized using ρ, g, and d to yield

$$E_f^* = \frac{E_f}{\rho(g^3 d^5)^{1/2}} \qquad (25)$$

Figure 3 shows linear and non-linear values of E_f^* for H/d = 0.6 and d/L in the range $0.05 \le d/L \le 0.18$. The linear wave power decreases monotonically with increasing d/L, however the non-linear variation rises to a maximum at a d/L value of approximately 0.095 and then decreases. The non-linear wave power is lower than the linear wave power by a margin of between 12% and 34%.

The results remaining to be presented concern the coupled wave/turbulent boundary layer calculation. Care has been taken in all cases to ensure that the Reynolds number $(\omega a^2/\nu)$ is sufficiently large as not to be a parameter of the flow. Consider first the wave friction factor which is normally defined in terms of the maximum bed shear stress (Equation (1)): in Figure 4, by contrast, f_w in defined in terms of phase-

averaged τ_b ($u_{0,max}$ is retained in the denominator). Highly pronounced asymmetry is seen in the variation of non-linear f_w: the maximum value exceeds the maximum linear value by 5%, but the magnitude of the largest negative value is greatly reduced by comparison with the linear value. (Note that the linear maximum is in close agreement with Equation (3).) The phase-averaged variation of f_e (which is distinct from the phase-averaged energy dissipation rate) is shown in Figure 5. A marked response to non-linearity is observed, the mean non-linear value being 72% lower than the mean linear value. Comparing Figures 4 and 5 it is seen that f_w(max.) is approximately equal to f_e(mean) in the linear case, whereas $f_e \ll f_w$ for the non-linear wave.

Returning now to the conventional definitions of f_w and f_e (Equations (1) and (2)), Figure 6 shows f_w for $a/k_s = 100$. The non-linear values depart from the linear case by between −12% and +8%, and broadly similar results (not shown) are obtained for $a/k_s = 30$ and 1000. It is in the results for f_e that the most dramatic effects of non-linearity are observed: Figures 7, 8, and 9 show the wave energy dissipation factor for $a/k_s = 30$, 100, and 1000. In all three cases f_e attains its lowest values in shallow water (smaller values of d/L) with higher waves (larger values of H/d). The distributions shown in Figures 7 to 9 may be compared with the computed linear values of $100f_e = 2.41$, 1.61, and 0.86, respectively.

Finally, the rate of wave energy dissipation as characterized by f_e is related to the non-dimensionalized wave power E_f^*. The reduction in wave power due to bed friction occurring over one wavelength, ΔE_f is equal to $(\overline{\tau_b.u_0})\,L$. Re-arrangement of Equations (2) and (25) leads to the following expression for the relative decrease in wave power per wavelength:

$$\frac{\Delta E_f}{E_f} = \left(\frac{2}{3\pi}\right)\left(\frac{u_{0,max}}{(gd)^{1/2}}\right)^3 \frac{1}{(d/L)}\,\frac{f_e}{E_f^*} \qquad (26)$$

Figure 10 shows $\Delta E_f/E_f$ for $H/d = 0.6$ and $a/k_s = 100$. The non-linear values are lower than the linear values by an approximately constant margin of 47%. This finding must, however, be considered in relation to Figure 3 which indicates than the power of the non-linear wave is less than that of its linear counterpart. Thus, while the non-linear wave transmits energy at a lower rate for given wave parameters, it also shows a lower proportional attenuation of that power.

5. CONCLUSIONS

Bed boundary layers have been computed using non-linear formulations for both the boundary layer and the driving wave motion. A novel aspect of the boundary layer treatment lies in the retention of the advective terms within a 1-D spatial discretization. Application of the non-linear wave theory developed by Rienecker and Fenton (1981) indicates that the power associated with a non-linear wave is significantly less than that of a linear wave with the same parameters. Non-linearity causes major reductions to occur in the wave energy dissipation factor, and it is found that the relative decrease in wave power per wavelength is considerable less than in a non-linear wave. It follows that, although a non-linear wave may have a lower 'initial' wave power, the relative decrease in that power per cycle is also lower.

Acknowledgement

Mrs. V. Moorhouse took appreciated care in preparing the present camera-ready manuscript.

REFERENCES

Brereton, G.J., and Mankbadi, R.R., 1995, "Review of recent advances in the study of unsteady turbulent internal flows", *Appl. Mech. Rev.*, Vol. 48, pp.189-212.

Buss, G.Y., and Stansby, P.K., 1982, "SAWW – A computer program to calculate the properties of steady water waves", Report, School of Engineering, University of Manchester.

Fredsøe, J., 1984, "Turbulent boundary layer in wave-current motion", ASCE *J. Hydraulic Engineering*, Vol. 110, pp.1103-1120.

Fredsøe, J., and Deigaard, R., 1992, *Mechanics of coastal sediment transport*, Advanced Series on Ocean Engineering, Volume 3, World Scientific, Singapore.

Justesen, P., 1988, "Prediction of turbulent oscillatory flow over rough beds", *Coastal Engineering*, Vol. 12, pp.257-284.

Kamphius, J.W., 1975, "Friction factor under oscillatory waves", ASCE *J. Waterways, Harbors, and Coastal Engineering Division*, Vol. 101, No. WW2, pp.135-144.

Nielsen, P., 1992, *Coastal bottom boundary layers and sediment transport*, Advanced Series on Ocean Engineering, Volume 4, World Scientific, Singapore.

Rienecker, M.M., and Fenton, J.D., 1981, "A Fourier approximation method for steady water waves", *J. Fluid Mech.*, Vol. 104, pp.119-137.

Rodi, W., 1993, *Turbulence models and their application in hydraulics. A state-of-the-art review*, 3rd ed., Balkema, Rotterdam.

Sajjadi, S.G., and Aldridge, J.N., 1995, "Prediction of turbulent flow over rough asymmetrical bed forms", *Appl. Math. Modelling*, Vol. 19, pp.139-152.

Schlichting, H., 1979, *Boundary-layer theory*, 7th ed., McGraw-Hill, New York.

Stansby, P.K., 1997, "Semi-implicit finite volume shallow-water flow and solute transport solver with k-ε turbulence model", *Int. J. Num. Meth. Fluids*, Vol. 25, pp.285-313.

Tanaka, H., Yamaji, H., and Sana, A., 1998, "Experimental study on non-linear wave boundary layers", Paper No. 274, *Book of Abstracts, 26th Int. Conf. on Coastal Engineering*, Copenhagen, pp.548-549.

Symbols (not defined in text)

c	wave speed, L/T
g	acceleration due to gravity
k	turbulent kinetic energy
p	pressure
P	rate of production of k

t	time
u_τ	friction velocity, $(\tau_b/\rho)^{1/2}$
z^+	zu_τ/ν
α,α_n	velocity amplitudes
ε	rate of dissipation of k
κ	wavenumber, $2\pi/L$; von Kármán constant
ν	kinematic viscosity
ν_t	turbulent kinematic viscosity
ρ	density
ω	angular frequency, $2\pi/T$

Subscripts

b	bed value
max	maximum
0	free stream value
1	first velocity node
1(t)	first turbulence node

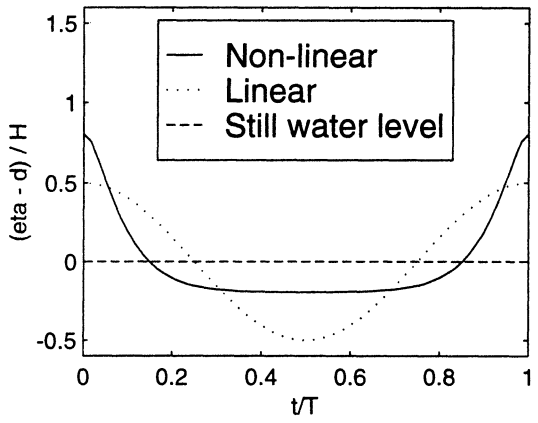

Figure 1. Wave profiles (H/d=0.6 , d/L=0.075)

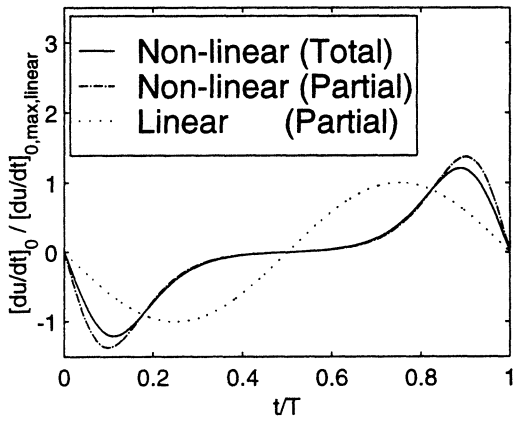

Figure 2. Wave acceleration at the bed (H/d=0.6 , d/L=0.075)

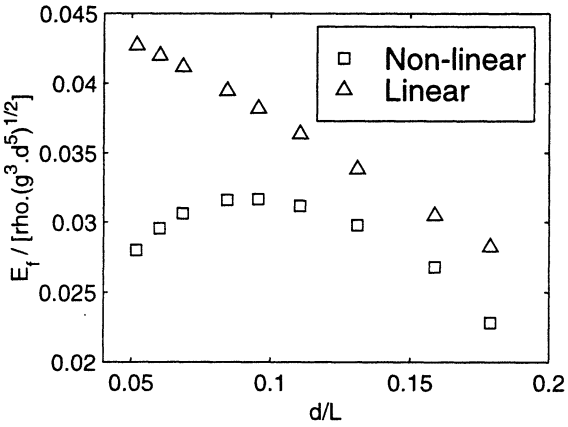

Figure 3. Normalized wave power (H/d=0.6)

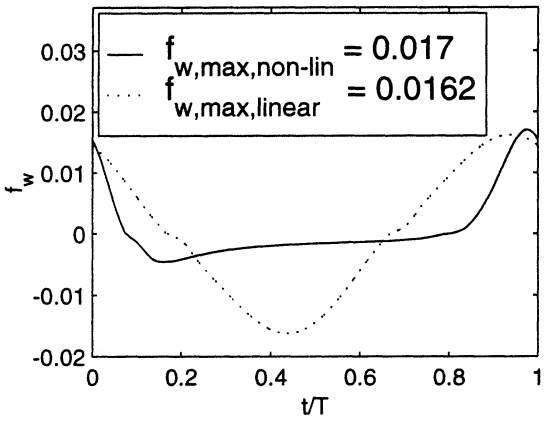

Figure 4. Phase-averaged wave friction factor (a/k_s=100 , H/d=0.6 , d/L=0.0518)

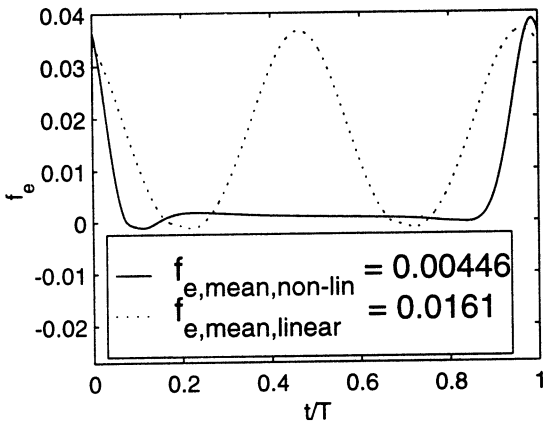

Figure 5. Phase-averaged wave energy dissipation factor (a/k_s=100 , H/d=0.6 , d/L=0.0518)

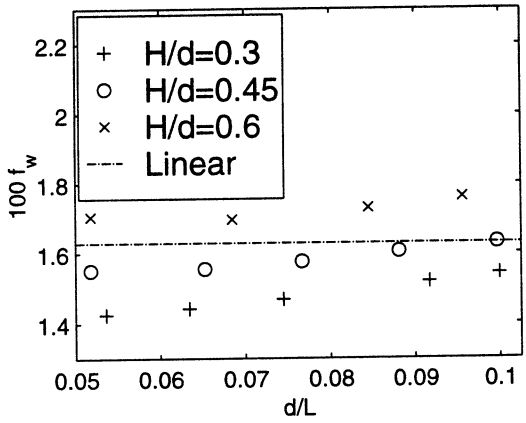

Figure 6. Wave friction factor, a/k_s=100

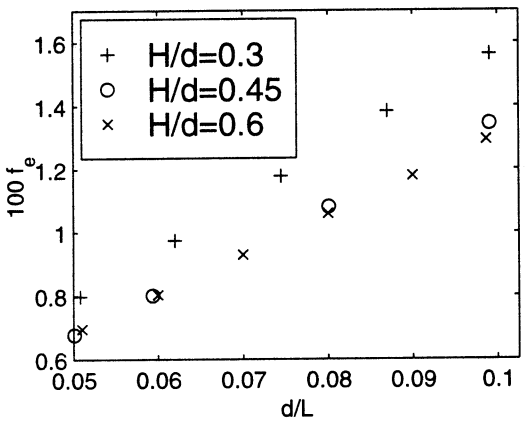

Figure 7. Wave energy dissipation factor, a/k_s=30

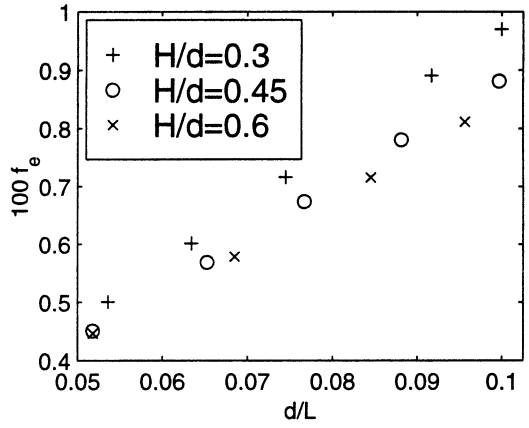

Figure 8. Wave energy dissipation factor, a/k_s=100

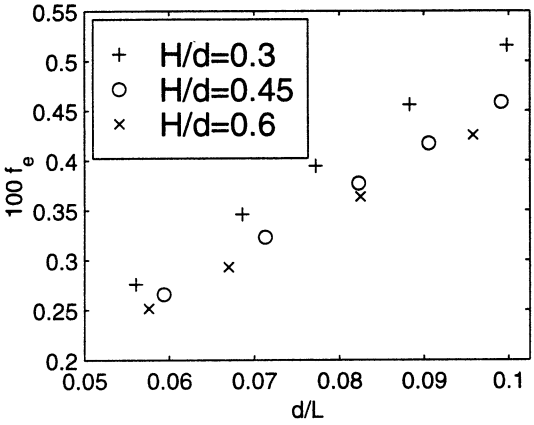

Figure 9. Wave energy dissipation factor, a/k_s=1000

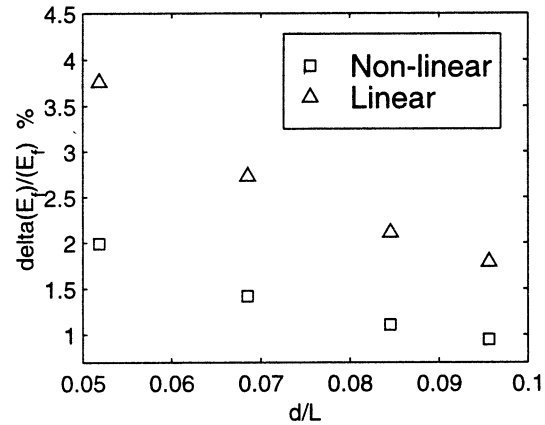

Figure 10. Relative decrease in wave power per wavelength (H/d=0.6 , a/k_s=100)